

**Cell Reports Methods, Volume 2**

**Supplemental information**

**Miniaturized and multiplexed high-content  
screening of drug and immune sensitivity  
in a multichambered microwell chip**

**Niklas Sandström, Valentina Carannante, Karl Olofsson, Patrick A. Sandoz, Elisabeth L. Moussaud-Lamodière, Brinton Seashore-Ludlow, Hanna Van Ooijen, Quentin Verron, Thomas Frisk, Madoka Takai, Martin Wiklund, Päivi Östling, and Björn Önfelt**

## Supporting Information

# Miniaturized and multiplexed high-content screening of drug and immune sensitivity in a multichambered microwell chip

### Author list and affiliations

Niklas Sandström<sup>\*1</sup>, Valentina Carannante<sup>\*1,2</sup>, Karl Olofsson<sup>1</sup>, Patrick A. Sandoz<sup>1</sup>, Elisabeth L. Moussaoud-Lamodière<sup>3</sup>, Brinton Seashore-Ludlow<sup>3</sup>, Hanna Van Ooijen<sup>1</sup>, Quentin Verron<sup>1</sup>, Thomas Frisk<sup>1</sup>, Madoka Takai<sup>4</sup>, Martin Wiklund<sup>1</sup>, Päivi Östling<sup>3</sup> and Björn Önfelt<sup>1,2</sup>

*\*Contributed equally*

1. Department of Applied Physics, Science for Life Laboratory, KTH Royal Institute of Technology, 171 65 Solna, Stockholm, Sweden

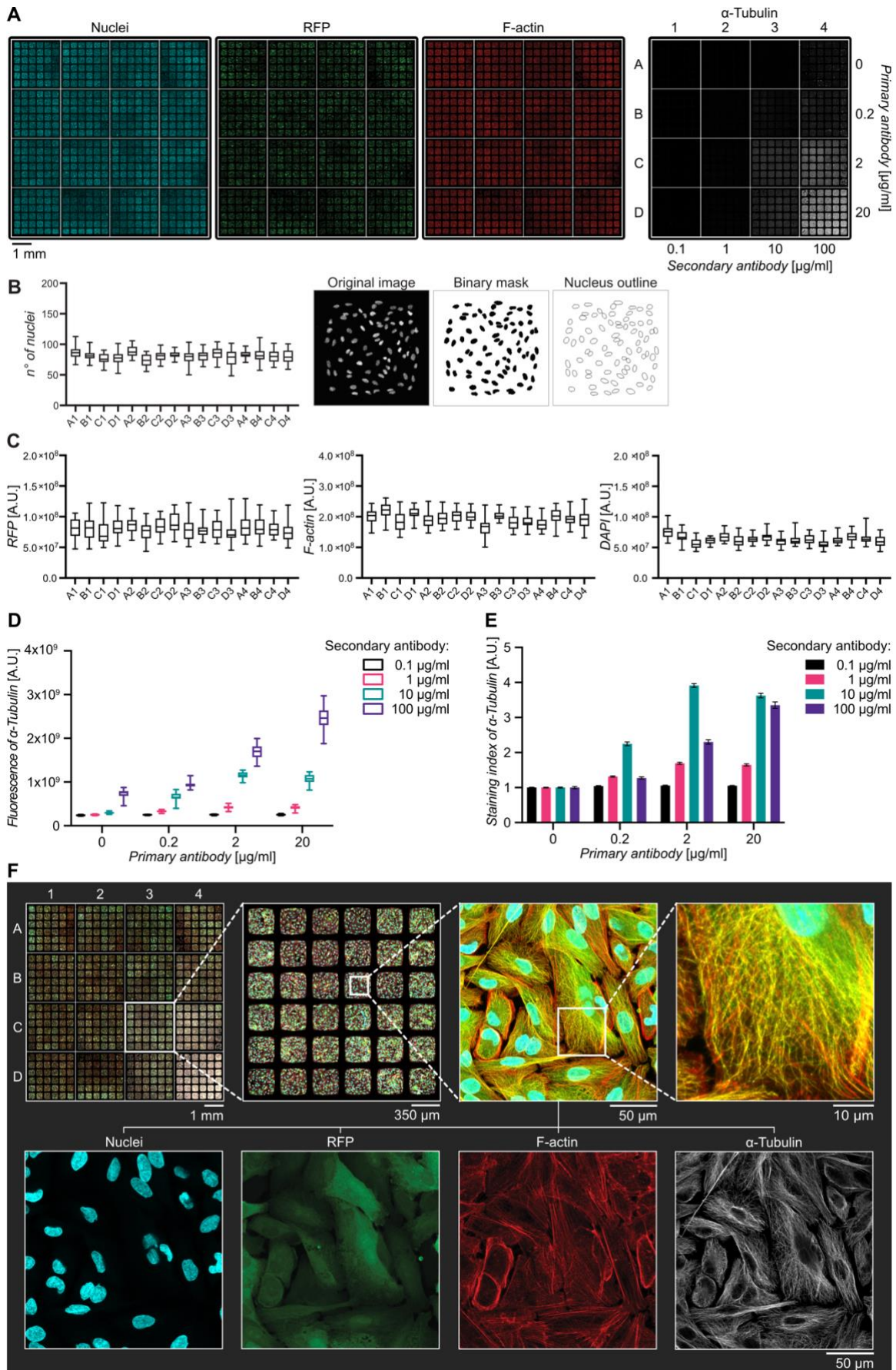
2. Department of Microbiology, Tumor and Cell Biology, Science for Life Laboratory, Karolinska Institutet, 171 65 Solna, Stockholm, Sweden

3. Department of Oncology and Pathology, Science for Life Laboratory, Karolinska Institutet, 171 65 Solna, Stockholm, Sweden

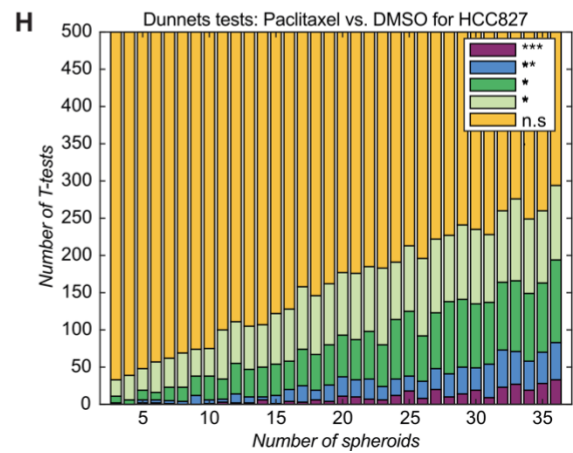
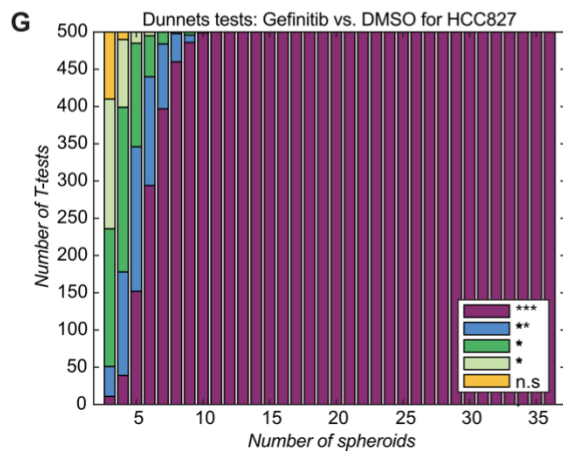
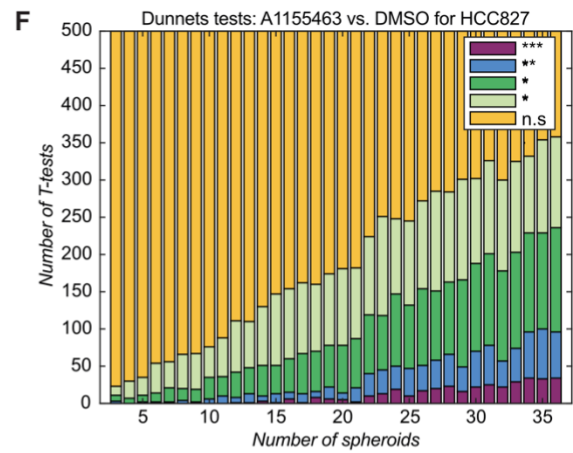
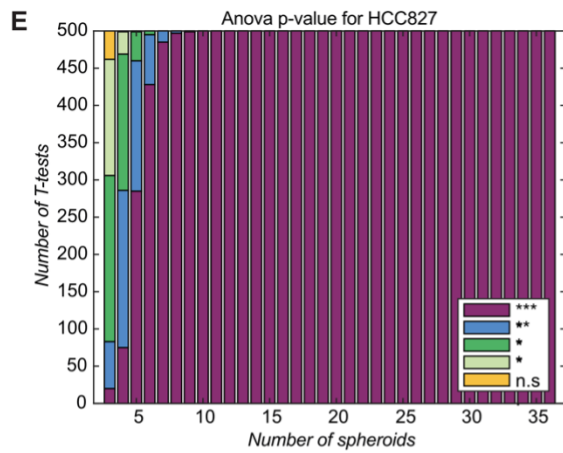
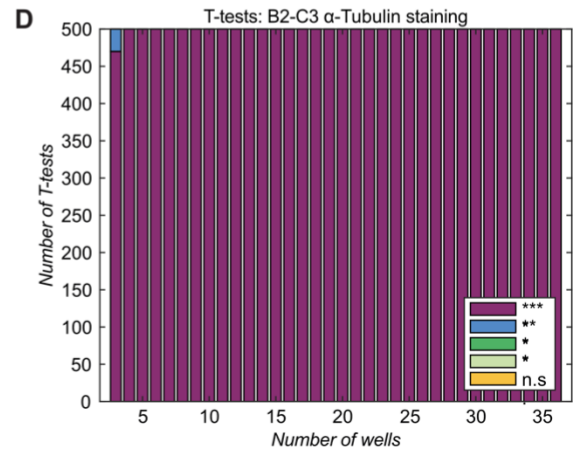
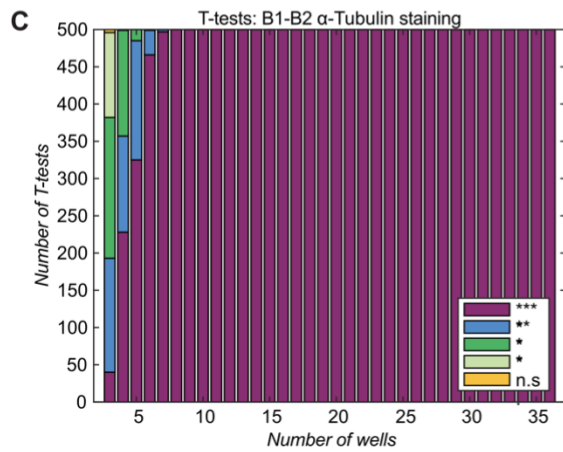
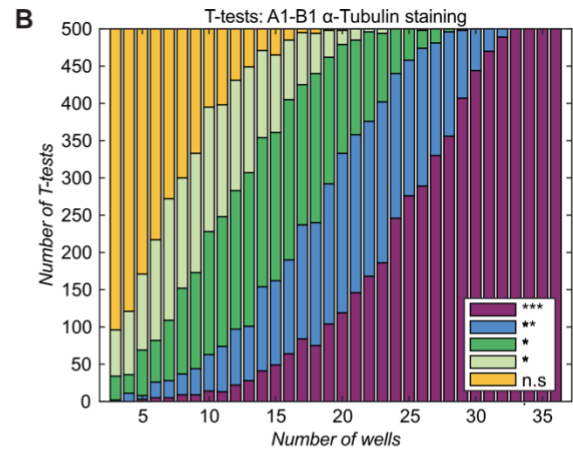
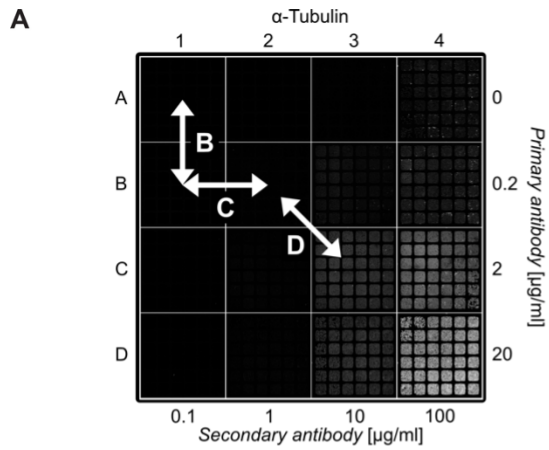
4. Department of Bioengineering, University of Tokyo, 7-3-1 Hongo, Bunkyo-Ku, Tokyo 113-8656, Japan.

**Lead contact:** Björn Önfelt

**Correspondence:** [Onfelt@kth.se](mailto:Onfelt@kth.se)

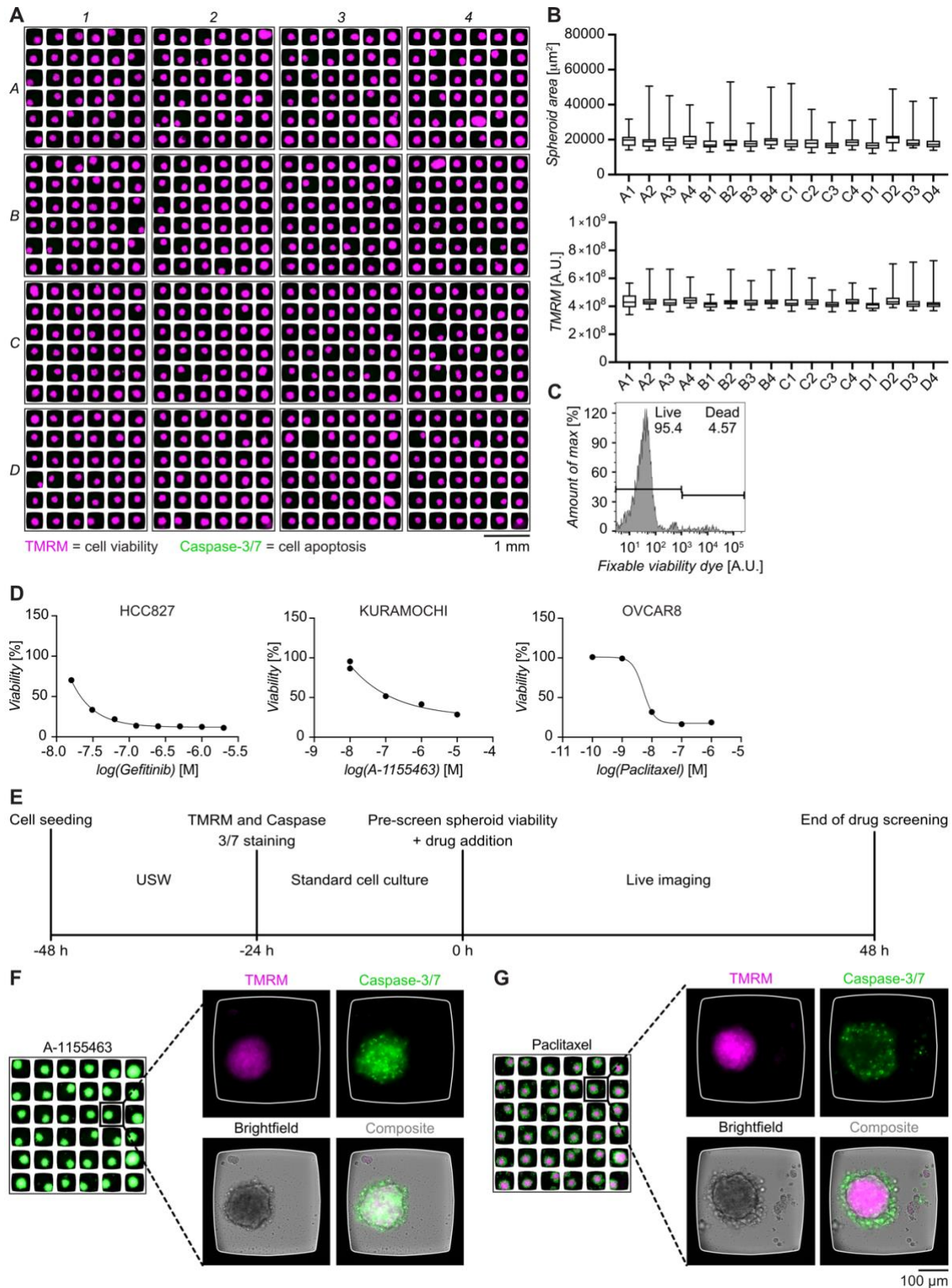


**Supplemental Figure S1, related to Figure 2.** Titration of antibodies for multiplex staining of monolayer cell cultures. **A)** Mosaic image of the entire microchip containing A498 RFP cells in each chamber. From left to right: DAPI (nuclei, cyan), RFP (cytoplasm, green), phalloidin (F-actin, red) and  $\alpha$ -tubulin (microtubules, grey). Increasing concentrations of primary antibody mouse anti-human anti- $\alpha$ -tubulin (from top to bottom: 0  $\mu\text{g/ml}$ ; 0.2  $\mu\text{g/ml}$ ; 2  $\mu\text{g/ml}$ ; 20  $\mu\text{g/ml}$ ) and secondary antibody donkey anti-mouse Alexa Fluor 647 (from left to right: 0.1  $\mu\text{g/ml}$ ; 1  $\mu\text{g/ml}$ ; 10  $\mu\text{g/ml}$ ; 100  $\mu\text{g/ml}$ ) were used to stain microtubules ( $\alpha$ -tubulin, right) across the different chambers, before the microchip was screened by confocal microscopy (10x objective) **B)** Left: Numbers of cell nuclei in the wells for the individual chambers. The box-and-whiskers graph is based on mean values from the three independent experiments where all 36 wells per chamber were analyzed. Two-way ANOVA with Tukey's Post Hoc Test revealed no significant differences in nuclei number between wells and chambers. Right: Example of a DAPI image from a single well, the corresponding binary mask and nuclei outlines after image analysis. A watershed algorithm was applied to separate adjacent nuclei and the number of nuclei was counted by the "Analyze particle" plugin of ImageJ. **C)** Total intensity of RFP, F-actin and DAPI from the 36 wells in each chamber of the microwell chip for three independent experiments. Two-way ANOVA with Tukey's Post Hoc Test revealed no significant differences in RFP, F-actin and DAPI signal between wells and chambers. **D)** Fluorescence signal from  $\alpha$ -tubulin (Alexa Fluor 647) in the 36 wells for each primary and secondary antibody combination. **E)** Staining index, assessing signal-to-noise ratio, for each antibody combination. Columns represent mean values from 36 individual wells and error bars represent the standard error of the mean (SEM). **F)** First row: composite images with increasing zoom and magnification. From left to right: mosaic image of the entire multichambered microwell chip, followed by a closer view of the entire C3 chamber (both acquired at 10x magnification). A single well of the C3 chamber imaged at higher magnification (40x objective) showing filaments and nuclei at the cellular level, followed by a cropped and enlarged view to visualize the same structures at the subcellular level. Second row: each fluorescence channel from the indicated image presented separately with nuclei (cyan), F-actin (red), RFP (green) and  $\alpha$ -tubulin (grey). All box and whisker plots show median values, while the box represents 25<sup>th</sup> to the 75<sup>th</sup> percentiles and the bars the minimum and maximum values.



**Supplemental Figure S2, related to Figure 2 and 3.** Examples showing how the number of analyzed wells correlate with statistical significance. A MATLAB script was designed to perform 500 statistical tests between samples containing  $n=3-36$  randomly picked wells from the different conditions to be compared. The same well could be picked multiple times within a sample. Columns in the graphs shown in panels B-H represent the outcomes of the 500 statistical tests performed for each value of  $n$ . The colors indicate the statistical power (light green ( $*p \leq 0.05$ ), green ( $**p \leq 0.01$ ), blue ( $***p \leq 0.001$ ) and purple ( $****p \leq 0.0001$ ) or non-significant (yellow). **A)** Mosaic overview of the tubulin immunostaining titration shown in Figure S1A with arrows B, C and D indicating the pairs of chambers of the chip that were tested in panels B-D below. **B-D)** Graphs showing statistical outcome from comparison of samples with  $n=3-36$  wells evaluated by two sample t-tests comparing chambers A1 and B1 (B), B1 and B2 (C) and B2 and C3 (D). **E-H)** Graphs showing statistical outcome by one-way ANOVA followed by Dunnett's Post Hoc test from comparison of samples with  $n=3-36$  wells for the log-transformed HCC827 total apoptosis data from Figure 3E. Overall comparison by one-way ANOVA (E), or individual comparisons by Dunnett's between A1155463 and DMSO (F), Gefitinib and DMSO (G) and Paclitaxel and DMSO (H). Overall this picture highlights that the number of wells needed to reach statistical significance vary depending on the conditions that are compared. For some conditions (e.g. panels C-E, G) only a few wells ( $<10$ ) are needed to reach significance, while for other samples (e.g. F and H) significance is not reached in all combination of samples even for  $n=36$ .



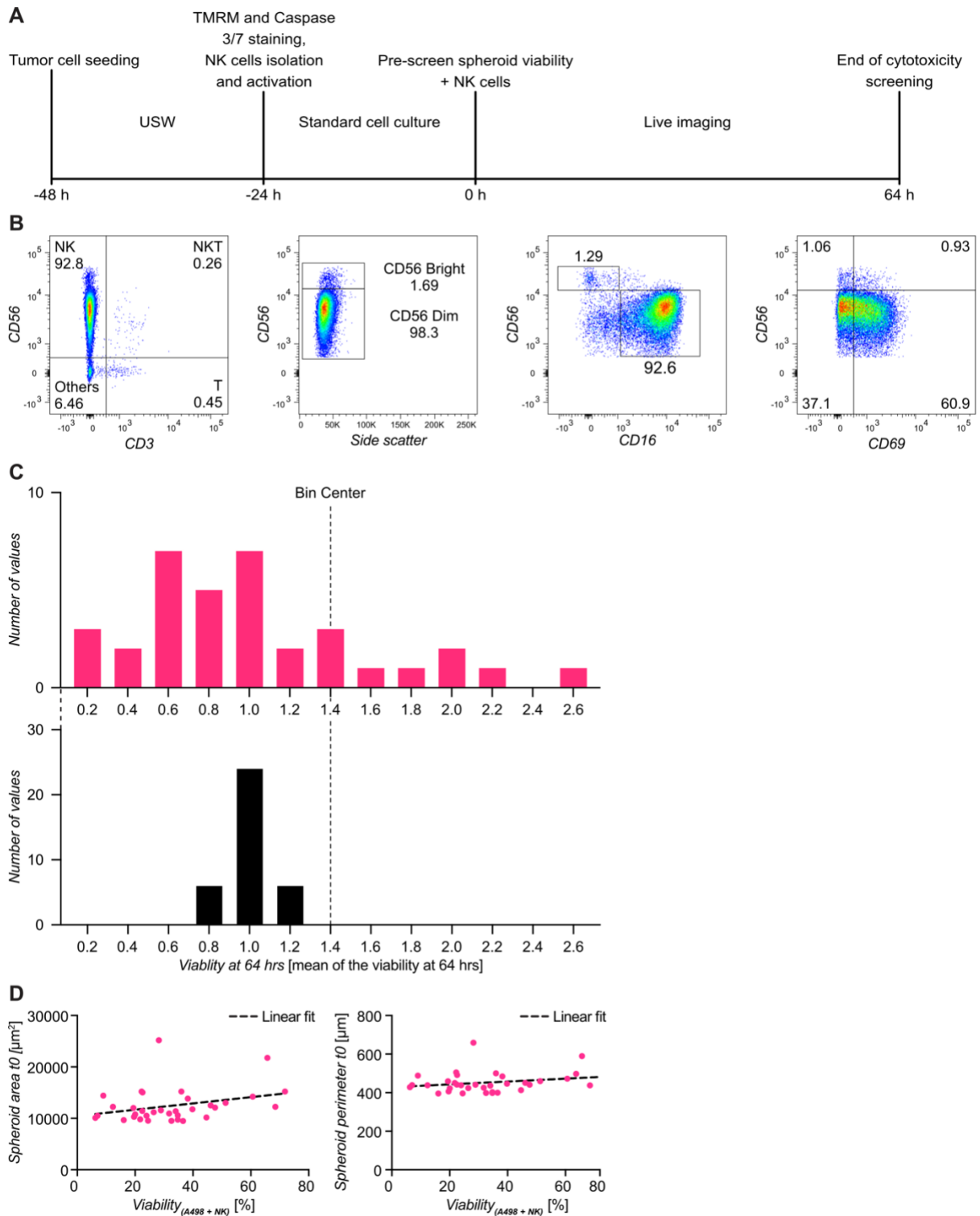


**Supplemental Figure S3, related to Figure 3.** A) Tumor spheroid preparation and experimental design for 3D drug screening assay. A) Mosaic image of USW-induced A498 spheroids in the multichambered microwell chip showing formation of live spheroids in each well across the chip. TMRM (magenta) and Caspase-3/7 (green) were used as markers of viability and apoptosis. B) USW-induced A498 spheroids from three different experiments were characterized in term of size and TMRM intensity. No significant differences in spheroid area and TMRM intensity were detected in Two-way ANOVA with Tukey's Post Hoc tests. Box and whisker plots show median values, while the box represents 25<sup>th</sup> to the 75<sup>th</sup> percentiles and the bars the minimum and maximum values. C)

Analysis of cell viability performed by flow cytometry on A498 cells obtained from USW-induced spheroids after enzymatic dissociation. **D)** Drug-response curves of HCC827, Kuramochi and OVCAR8 to gefitinib, A-1155463 and paclitaxel respectively. Data were extracted from a larger experiment where drug sensitivity was measured by exposing cells to a small molecule library consisting of 528 drugs pre-plated in 384-well plates, where each well contained one drug at a certain concentration, for 72 hours. These 528 oncology drugs belong to a library of Institute for Molecular Medicine Finland (FIMM), which contain oncology drugs that are clinically approved or under investigation. The viability of cells was measured with CellTiter-Glo (Promega, G7570) at 72 hours. Drug response curves were fitted after per plate normalization using Breeze (<https://www.fimm.fi/en/software-tools>)\* yielding a Drug Sensitivity Score (DSS) for each drug-cell line pair. **E)** Schematic description of the 3D live-imaging drug toxicity assay. 48 hours before the beginning of the assay, tumor cells were seeded in the multichambered microwell chip and exposed to ultrasounds to induce cell aggregation. After 24 hours, the USW was turned off, TMRM and Caspase-3/7 were added and the tumor spheroids were left to develop and take up the dye for 24 hours. At the day of the assay, images of A498 spheroids were acquired to evaluate viability and size before the addition of drugs. After the addition of each treatment, the microwell chip was transferred into a widefield microscope equipped with an incubation chamber to perform live imaging for 48 hours acquiring one frame every four hours. **F)** Chamber containing OVCAR8 spheroids after 48 hours incubation with A-1155463 (left) and one representative tumor spheroid showing the distribution of TMRM and Caspase-3/7 signal in the spheroid (right). Apoptotic cells (green) were uniformly distributed in the tumor spheroids. **G)** Chamber containing OVCAR8 spheroids after 48 hours incubation with paclitaxel (left) and one representative spheroid showing the distribution of TMRM and Caspase-3/7 signal in the spheroid (right). Apoptotic cells were located at the periphery of the tumor spheroid.

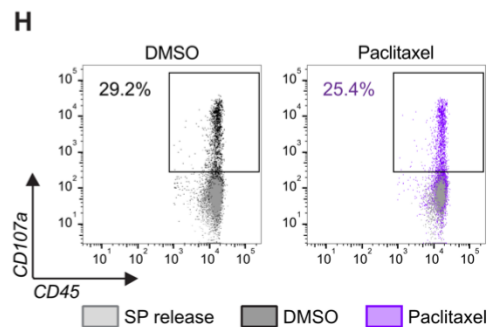
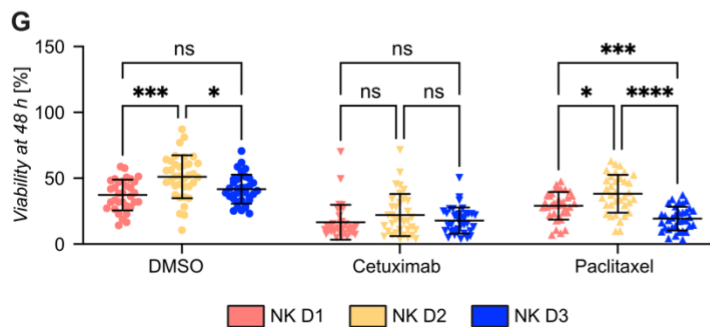
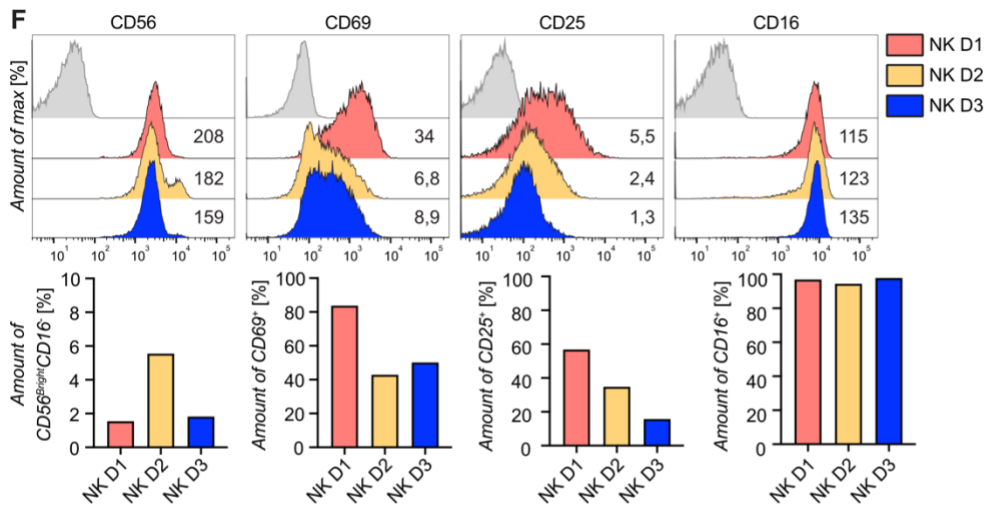
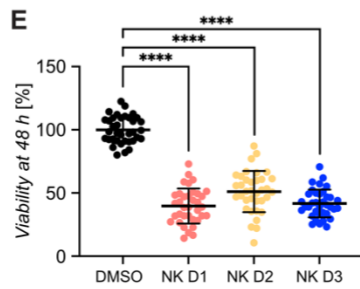
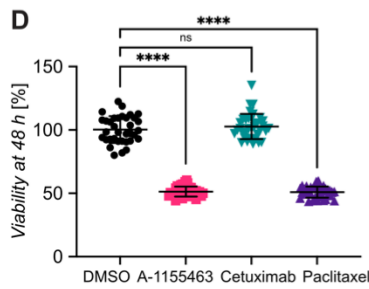
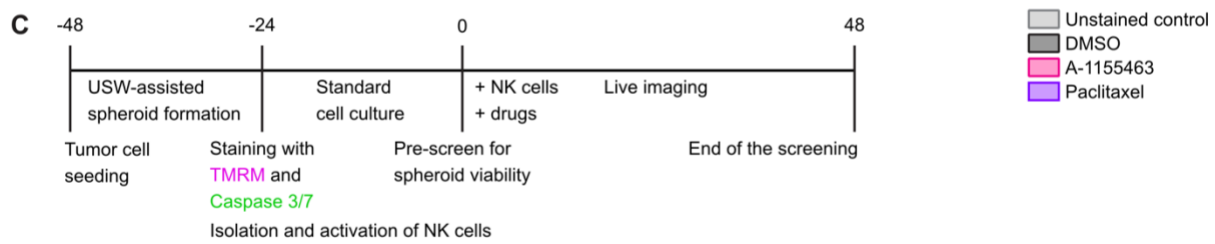
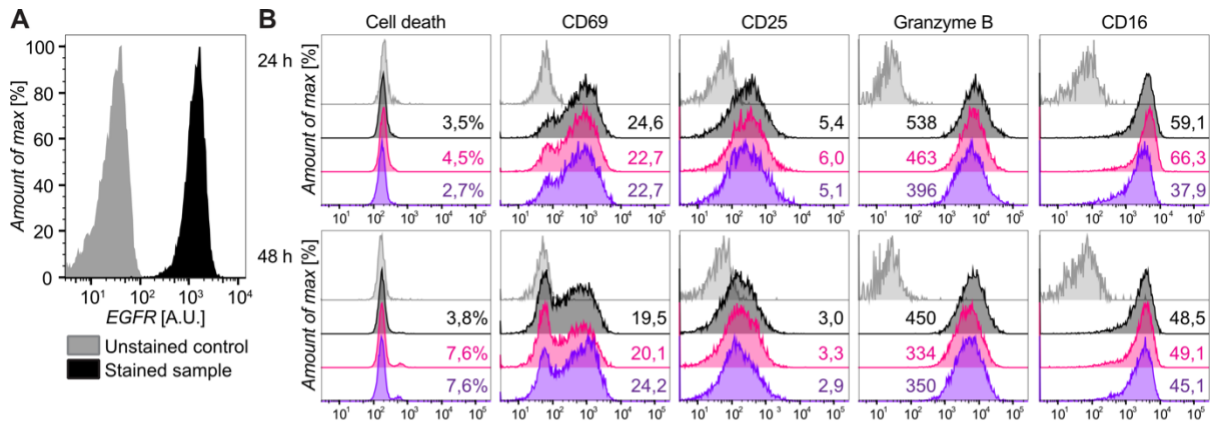
\* Potdar, S. et al. Breeze: An integrated quality control and data analysis application for high-throughput drug screening. *Bioinformatics* **36**, 3602–3604 (2020).



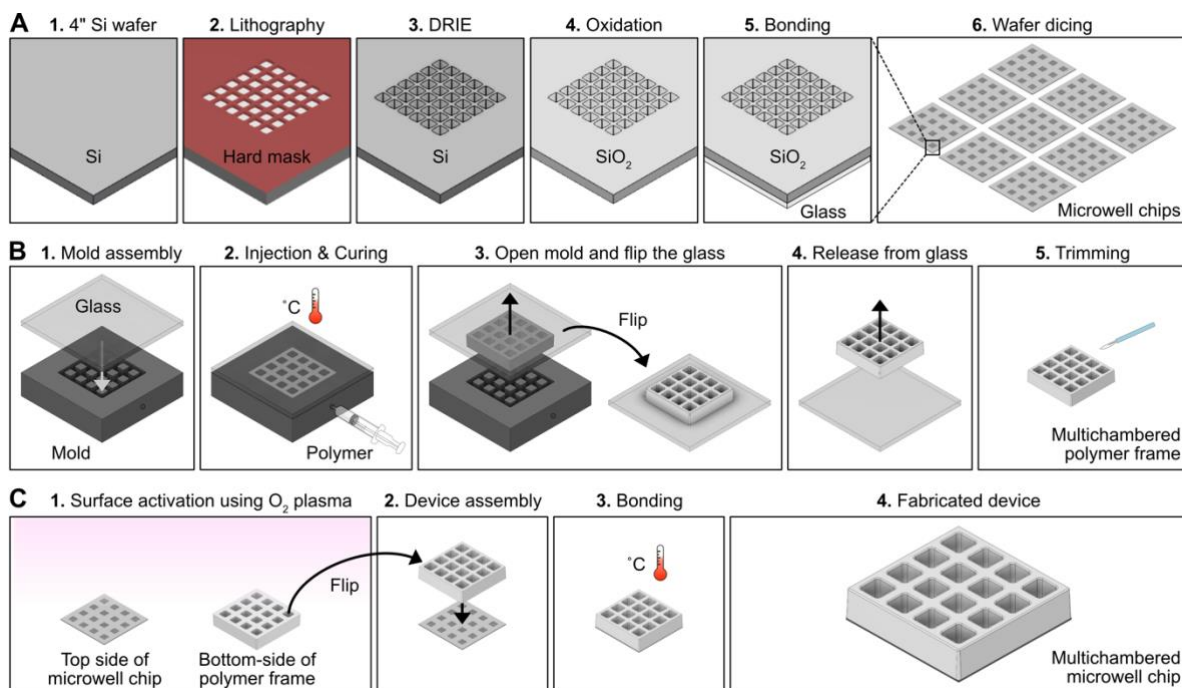


**Supplemental Figure S4, related to Figure 4.** Experimental design of the NK cell cytotoxicity screening assay, NK cell characterization and correlation between spheroid size and NK cell response. **A)** Schematic description of the 3D live-imaging NK cells cytotoxicity assay. 48 hours before the beginning of the assay, tumor cells were seeded in the multichambered microwell chip and exposed to ultrasounds to induce cell aggregation. After 24 hours, the USWs were turned off, TMRM and Caspase-3/7 were added and the tumor spheroids were left to develop and take up the dye for 24 hours. In parallel with turning off the USWs and adding dyes, NK cells were isolated from healthy donors and activated with IL-15 (10 ng/ml) overnight. At the day of the NK cell cytotoxicity assay, images of A498 spheroids were acquired to evaluate viability and size before the addition of NK cells. NK cells were collected, resuspended in fresh culture medium and added at a concentration of 20 000 cells/chamber while only fresh culture medium was added to the control chamber. After the addition of NK cells, the

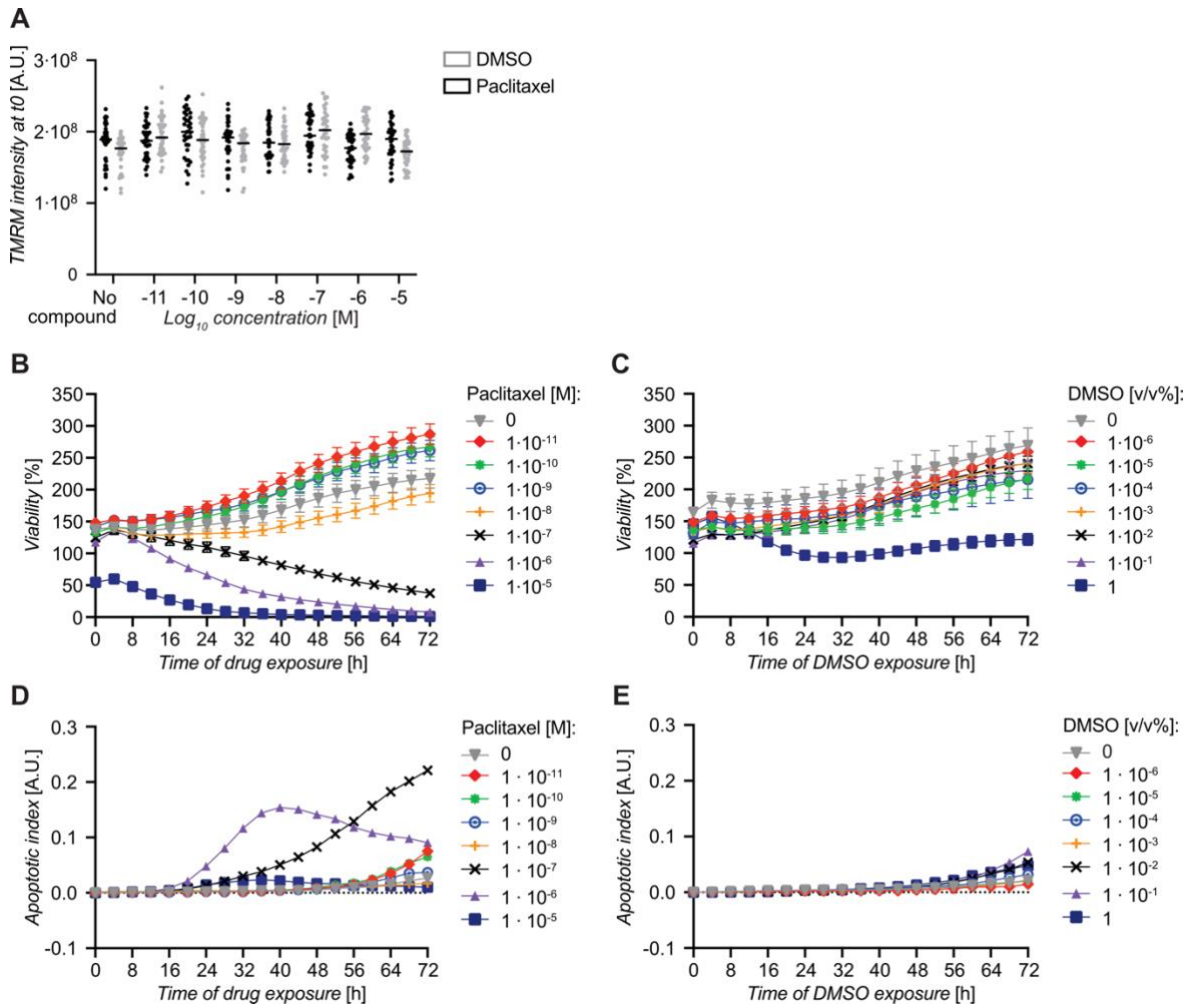
multichambered microwell chip was transferred into a widefield microscope equipped with an incubation chamber to perform live imaging for 64 hours acquiring one frame every four hours. **B)** Flow cytometry analysis of NK cells after isolation from buffy coats. NK cells (defined as CD56<sup>+</sup>CD3<sup>-</sup>) represented 92.8% of the cells isolated from the donor used in the assay. This NK cell population was characterized by a relatively high fraction of CD56<sup>Dim</sup> (98,3%) NK cells, most of them positive for CD16 and approximately 60% of them expressing the activation marker CD69. **C)** Histogram showing heterogeneity in viability between individual A498 spheroids incubated with (top) or without (bottom) NK cells for 64 hours. The viability measured for each spheroid has been divided by the mean viability of the corresponding condition. The larger spread for A498 spheroids incubated with NK cells is indicative of larger heterogeneity in cytotoxic response between microwells. **D)** Analysis of the correlation between spheroid viability in response to NK cells and spheroid area (left) and spheroid perimeter (right) at timepoint 0. No significant correlation was found as indicated by low R squared values of  $R^2 = 0.09$  (left panel) and  $R^2 = 0.23$  (right panel).



**Supplemental Figure S5, related to Figure 5.** Phenotypic characterization, experimental design and responses in the combinatorial drug/NK cytotoxicity screening assay. **A)** Flow cytometry histogram of EGFR expression on OVCAR8 cells (black) compared to unstained control (light grey). **B)** Phenotype of NK cells exposed to drugs analyzed by flow cytometry. NK cells were exposed to DMSO (dark grey), 10  $\mu$ M of A-1155463 (magenta) or 1  $\mu$ M of paclitaxel (purple) for 24 hours (upper panel) or 48 hours (lower panel). Unstained control shown in light grey. Indicated percentages of dead cells and relative mean fluorescent intensity values for the molecular markers have been calculated for NK cells (cells gated on CD56<sup>+</sup>CD3<sup>-</sup>). **C)** Schematic description of the 3D live-imaging combinatorial drug/NK cells cytotoxicity assay. 48 hours before the beginning of the assay, OVCAR8 tumor cells were seeded in the multichambered microwell chip and exposed to ultrasounds to induce cell aggregation. After 24 hours, the USWs were turned off, TMRM and Caspase-3/7 were added and the tumor spheroids were left to develop and take up the dye for 24 hours. In parallel with turning off the USWs and adding dyes, NK cells were isolated from healthy donors and activated with IL-15 (10 ng/ml) overnight. At the day of the assay, images of OVCAR8 spheroids were acquired to evaluate viability and size before the addition of NK cells. NK cells were collected, resuspended in fresh culture medium and added at a concentration of 20 000 cells/chamber together with the drugs while only fresh culture medium was added to the control chamber. After the addition of NK cells and drugs, the microwell chip was transferred to a widefield microscope equipped with an incubation chamber to perform live imaging for 48 hours acquiring one frame every four hours. **D)** Viability of OVCAR8 spheroids cultured with DMSO (black), 10  $\mu$ M of A-1155463 (magenta), 10  $\mu$ M of cetuximab (teal) or 1  $\mu$ M of paclitaxel (purple) in the absence of NK cells. One-way ANOVA with Dunnett's Post Hoc Test revealed significant differences in OVCAR8 viability after A-1155463 and paclitaxel treatment compared to DMSO control (n=36, \*\*\*\*p  $\leq$  0.0001; ns, not-significant). **E)** Viability of OVCAR8 spheroids cultured alone (black) with NK cells from donor 1 (orange), donor 2 (yellow) or donor 3 (blue) in presence of DMSO but no drugs. One-way ANOVA with Dunnett's Post Hoc Test revealed significant differences in OVCAR8 viability after exposure to NK cells from all donors compared to DMSO control (n=36, \*\*\*\*p  $\leq$  0.0001). **F)** Flow cytometry analysis of NK cells (CD56<sup>+</sup>CD3<sup>-</sup>) before being used in the 3D killing assay. Top: histograms showing expression levels and relative mean fluorescent intensity for the indicated molecular markers from donor 1 (orange), donor 2 (yellow), donor 3 (blue) and unstained controls (grey). Bottom: Bar graphs showing percentage of NK cells expressing the indicated molecular markers. Color scheme as above. **G)** Viability of OVCAR8 spheroids cultured with NK cells from donor 1 (orange), donor 2 (yellow) or donor 3 (blue) in presence of DMSO (round dots), 10  $\mu$ M of cetuximab (inverted triangles) or 1  $\mu$ M of paclitaxel (triangle). Mixed model ANOVA with Tukey's Post Hoc Test revealed significant differences between donors in term of drug responses (n=36, \*p  $\leq$  0.05; \*\*\*\*p  $\leq$  0.0001; ns, not-significant). **H)** NK cells activated overnight with IL-15 were exposed to DMSO (left, black dots) or 1  $\mu$ M of paclitaxel (right, purple dots) for 48 hours before being used in a 4-hour CD107a degranulation assay. Spontaneous CD107a release (SP release) is shown in light grey in both plots. The percentages of cells showing specific release (CD107a release above the threshold given by the SP release) are indicated in each plot.



**Supplemental Figure S6, related to Figure 1.** Fabrication schemes for the multichambered microwell chip. **A)** Fabrication of the Si-glass microwell chips (steps 1-6). Note, the illustrations show a single microwell array from a small area of a single chip for a clear and detailed view, however, the fabrication was based on 4-inch wafers, which after dicing resulted in 9 microwell chips, as indicated in step (6). **B)** Manual reaction injection molding of multichambered polymer frames in structured molds (step 1-5). **C)** Surface activation and subsequent dry-bonding of Si-glass microwell chips with multichambered polymer frames (step 1-3). The assembled multichambered microwell chip is illustrated in (step 4).



**Supplemental Figure S7, related to Star Methods section “Image analysis of drug toxicity and killing”.** Example data used to for calculation of specific viability and specific apoptotic index. OVCAR8 cells were cultured in different concentrations of paclitaxel or DMSO for 72 hours. **A)** TMRM intensity from OVCAR8 cells in the microwell chip before addition of paclitaxel (black) or corresponding dilution of DMSO (grey). The dots represent the intensities from the 36 individual microwells in each chamber and the black bars are mean values. **B,C)** Time course of the viability of OVCAR8 cells exposed to different concentrations of paclitaxel (B) or corresponding dilutions of DMSO (C) for 72 hours. Viability is the TMRM signal normalized to the TMRM signal at timepoint 0 (before addition of drug or DMSO). Symbols corresponds to mean values from the 36 microwells and error bars are SEM. **D,E)** Time course of apoptotic index for OVCAR8 cells exposed to different concentrations of paclitaxel (D) or corresponding dilutions of DMSO (E) for 72 hours. The apoptotic index is the signal from Caspase-3/7 divided by the TMRM signal of the tumor cells at timepoint 0.